



Flywheel energy storage systems: Review and simulation for an isolated wind power system

R. Sebastián*, R. Peña Alzola

Department of Electrical, Electronic and Control Engineering, Spanish University for Distance Education, UNED, 28040 Madrid, Spain

ARTICLE INFO

Article history:

Received 28 March 2012

Received in revised form

3 August 2012

Accepted 4 August 2012

Available online 9 October 2012

Keywords:

Flywheel energy storage systems

Isolated power systems

Wind power

Wind diesel

Short-term simulation

ABSTRACT

In flywheel based energy storage systems (FESSs), a flywheel stores mechanical energy that interchanges in form of electrical energy by means of an electrical machine with a bidirectional power converter. FESSs are suitable whenever numerous charge and discharge cycles (hundred of thousands) are needed with medium to high power (kW to MW) during short-time periods (seconds–minutes). Monitoring of the FESS state of charge is simple and reliable as only the spinning speed is needed. The materials for the flywheel, the type of electrical machine, the type of bearings and the confinement atmosphere which all together determine the FESSs energy efficiency ($> 85\%$) are reviewed. Main FESS applications: power quality, traction and aerospace are presented. Additionally in this paper it is presented the simulation of an isolated wind power system (IWPS) consisting of a wind turbine generator (WTG), a consumer load, a synchronous machine (SM) and a FESS. A low-speed iron flywheel driven by an asynchronous machine (ASM) is sized for the presented IWPS. The simulation results with graphs for system frequency, system voltage, active powers of the different elements, and FESS-ASM speed, direct and quadrature currents are presented showing that the FESS effectively smoothes the wind power and consumer load variations.

© 2012 Elsevier Ltd. All rights reserved.

Contents

1. Introduction	6804
2. Components of the flywheel based energy storage systems	6804
2.1. Flywheel material	6805
2.2. Flywheel shape	6805
2.3. Electrical machine	6805
2.4. Power converter	6806
2.5. Bearings	6806
2.6. Enclosure	6806
2.7. FESS components research and development needs.	6806
3. FESS main applications	6807
3.1. Applications related to power quality.	6807
3.2. Applications related to traction.	6807
3.3. Applications related to aerospace industry.	6807
4. Application of a FESS to an isolated wind power system.	6807
5. IWSP with FESS simulation schematics.	6808
5.1. FESS description and sizing	6808
6. IWPS with FESS simulation results	6810
6.1. Load step	6810
6.2. Wind step.	6811
7. Conclusions	6812
References	6812

* Corresponding author.

E-mail address: rsebastian@ieec.uned.es (R. Sebastián).

1. Introduction

Flywheel energy storage systems (FESSs) store mechanical energy in a rotating flywheel that convert into electrical energy by means of an electrical machine and vice versa the electrical machine which drives the flywheel transforms the electrical energy into mechanical energy. Fig. 1 shows a diagram for the components that form a modern FESS. The flywheel, with moment of inertia I , spins at a speed ω storing kinetic energy E_c as

$$E_c = \frac{1}{2} I \omega^2 \quad (1)$$

Moment of inertia depends on the flywheel mass and geometry [1] as follows:

$$I = \int r^2 dm \quad (2)$$

where r is the distance of each differential mass element dm to the spinning axis.

The bi-directional power converter transforms electrical energy at the machine frequency into DC electrical energy and vice versa. Another bi-directional converter is necessary to transform DC electrical energy to AC electrical energy at grid frequency 50/60 Hz and vice versa.

Rated power determines the sizing of the electrical machine and the power converter. The duration of the energy interchange is determined by (1) and the rated power, neglecting losses.

FESSs are adequate for interchanging medium and high powers (kW to MW) during short periods (seconds) with high

energy efficiency ($> 85\%$) [2,3]. In these situations, FESSs have favorable characteristics when compared with electrochemical batteries. FESSs allow a very high number of charge/discharge cycles (hundreds of thousands). This number of cycles is independent of the temperature and the depth of the discharge (DOD). Therefore, the FESS useful lifetime is very long (> 20 years) and FESS disposal does not have environmental concerns. In addition, monitoring of the state of charge (SOC) for FESS is simple and reliable as only the flywheel spinning speed is needed to know [3]. Main applications of FESSs are related to power quality, traction and aerospace industry.

2. Components of the flywheel based energy storage systems

In order to maximize E_c , according to (1), moment of inertia I in (2) can be increased by increasing the flywheel volume (radius r and height) and the material mass m . Spinning speed ω can be also increased, which results in a greater efficiency as spinning speed is squared in (1).

Broadly speaking, the flywheel spinning speed ω allows classifying FESSs in two types [7]: low-speed FESSs (< 6000 rpm) and high-speed FESSs (10^4 – 10^5 rpm). In order to maximize the energy efficiency low-speed FESSs make use of conventional technologies, whereas high-speed FESSs make use of advanced technologies. For this reason, the price of low-speed FESSs can be up to five times lower than the cost of high-speed FESSs [7] although their performance is always inferior. Characteristics of both FESS types are described next and summarized in Table 1.

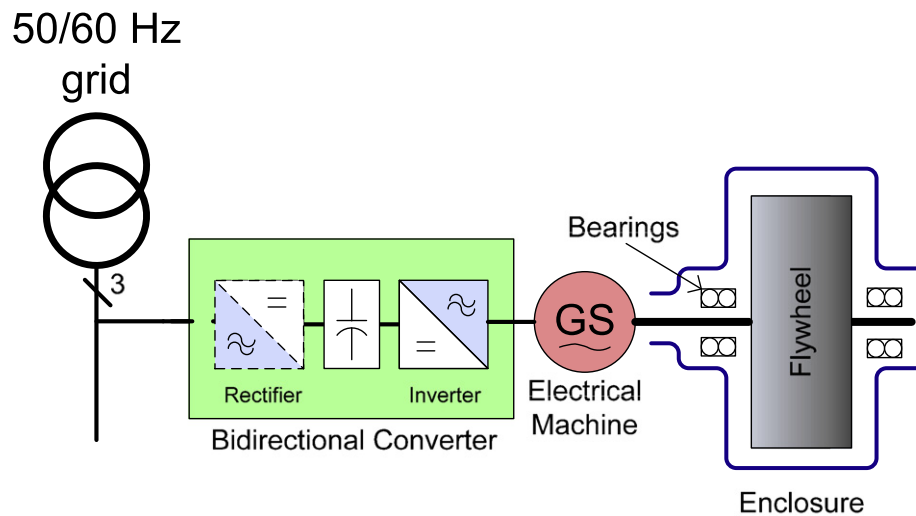


Fig. 1. Components that form an FESS.

Table 1
Characteristics of low-speed FESSs and high-speed FESSs.

Characteristic	Low-speed FESSs	High-speed FESSs
Flywheel material [4,5]	Steel	Composite materials: glass and carbon fibers
Electrical machine	Asynchronous, permanent magnet synchronous and reluctance machines	Permanent magnet synchronous and reluctance machines
Integration of electrical machine and flywheel [6]	No integration or partial integration	Full or partial integration
Confinement atmosphere [7]	Partial vacuum or light gas	Absolute vacuum
Enclosure weight [8]	$2 \times$ flywheel weight	$\frac{1}{2} \times$ flywheel weight
Bearings [7,4]	Mechanical or mixed (mechanical and magnetic)	Magnetic
Main applications	Power quality [4]	Traction and aerospace industry
Cost	1	5

2.1. Flywheel material

The maximum spinning speed ω is determined by the capacity of the material to withstand the centrifugal forces affecting the flywheel, that is, the material tensile strength [7].

Centrifugal forces are proportional to the mass, the radius and the squared spinning speed. The maximum energy per volume unit (energy density) and per mass unit (specific energy) are respectively [9]

$$e_v = K \sigma_{\theta,u} \quad (3)$$

$$e_m = K \frac{\sigma_{\theta,u}}{\rho} \quad (4)$$

where K is a constant depending on the shape, ρ is the mass density and $\sigma_{\theta,u}$ the maximum tensile strength. Table 2 compares all these mentioned characteristics for metallic and composite material usually employed in flywheels.

Table 2
Characteristics for different flywheel materials [10].

Material	ρ (kg/m ³)	$\sigma_{\theta,u}$ (MPa)	e_v (MJ/m ³)	e_m (kJ/kg)
Aluminum	2700	500	251	93
Steel	7800	800	399	51
Glass E/epoxy	2000	1000	500	250
Graphite HM/epoxy	1580	750	374	237
Graphite HS/epoxy	1600	1500	752	470

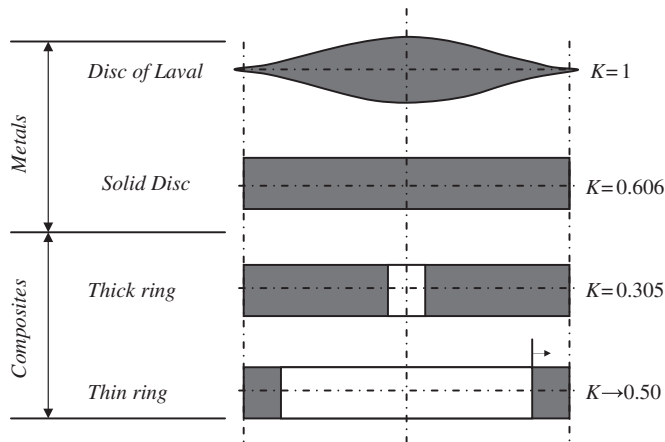


Fig. 2. Different flywheel shapes.

In order to obtain high specific energy, flywheel materials must be light, with low ρ , and have high tensile strength allowing high spinning speeds, such as modern composite materials. Metals are heavy and do not allow reaching high spinning speeds. Metals only allow obtaining modest energy density, but prices are 20/30 times lower than those of the composite materials [5].

2.2. Flywheel shape

Eqs. (3) and (4) are valid assuming axial symmetry and planar stress [11]. The shape factor K can be described as a measurement of the flywheel material utilization. Fig. 2 shows the main flywheel shapes used for metallic and composite materials and the values of K for the case of homogenous isotropic materials [11].

2.3. Electrical machine

The electrical machine, acting as a generator, slows down the flywheel transforming its mechanical energy into electrical energy. Conversely, the electrical machine, acting as motor, speeds up the flywheel increasing its mechanical energy and consuming electrical energy. Table 3 summarizes the main characteristics of the electrical machines suitable to be used for FESS.

Asynchronous machines are used for high power applications because of its rough construction, high torque and low cost [12]. Copper rotor losses exclude the asynchronous machine from using enclosures with absolute vacuum as cooling results difficult. This is because the absolute vacuum allows only heat transferring by radiation. Doubly fed asynchronous machines have also been used for FESS as they allow reducing the sizing of the power converter [13,14].

Permanent magnet synchronous machines (PMSMs) have become the most usual choice for FESSs due to their high efficiency. PMSMs have no rotor losses resulting suitable for confinements in vacuum. The so-called Hallbach array for the permanent magnets allows eliminating all the iron losses at the expense of lower magnetic flux and thus lower power [5,15]. Permanent magnets have concern of accidental demagnetization, which increases with temperature. In addition, permanent magnets have high price and low tensile strength.

In order to solve these disadvantages, variable reluctance machines (VRMs) for FESSs have been proposed. VRMs have no demagnetization concern as torque is exclusively due to the reluctance variation. Materials for the constructing reluctance machines have high tensile strength and low cost. VRM rotor losses due to the slots are low enough to allow confinement with absolute vacuum [16,17].

Table 3
Main characteristics of the electrical machines suitable to be used for FESS [18,19].

Machine	Asynchronous	Variable reluctance	Permanent magnet synchronous
Power	High	Medium and low	Medium and low
Specific power	Medium (≈ 0.7 kW/kg)	Medium (≈ 0.7 kW/kg)	High (≈ 12 kW/kg)
Rotor losses	Copper and iron	Iron due to slots	None
Spinning losses	Removable by annulling flux	Removable by annulling flux	Non-removable, static flux
Efficiency	High (93.4%)	High (93%)	Very high (95.2%)
Control	Vector control	Synchronous: vector control. Switched: DSP	Sinusoidal: vector control. Trapezoidal: DSP
Size	1.8 l/kW	2.6 l/kW	2.3 l/kW
Tensile strength	Medium	Medium	Low
Torque ripple	Medium (7.3%)	High (24%)	Medium (10%)
Maximum/ base speed	Medium (> 3)	High (> 4)	Low (< 2)
Demagnetization	No	No	Yes
Cost	Low (22€/kW)	Low (24€/kW)	High (38 €/kW)

In high-speed FESSs, the electrical machine and the flywheel are fully integrated forming a single compact element. In low-speed FESSs they are separated apart or just partially integrated in a common enclosure.

Maximum spinning speed determines maximum FESS energy storage, see (1). Nevertheless, it is not possible to harness all the stored energy, as this would require too high electrical torque. This is because the required interchange power is equal to torque times spinning speed. A minimum speed of a half the maximum speed, which requires doubling the torque, allows harnessing 75% of the stored energy [5].

2.4. Power converter

The FESS connects the electrical machine to a DC-link by means of a bidirectional power converter (DC/AC) normally referred as inverter, see Fig. 1. This inverter is most often a three-phase bridge of semiconductor switches [20] working as a voltage source inverter (VSI) controlled by pulse width modulation (PWM). The proper selection for the switches (MOSFET, IGBT, etc.) will depend on the blocking voltages and current capabilities as well as on the switching frequency. Higher switching frequency reduces the electrical machine current and torque ripple [5] and increases control bandwidth, but at the expense of increasing switching losses. Additional LC-based filters may be needed to connect the inverter and the electrical machine. This would be necessary to supply sinusoidal currents without ripple into the machine and thus reducing losses, windings deterioration and EMI [21,22]. The inverter is controlled to make the electrical machine behave as a generator or as a motor according to the instantaneous needs. Electrical machine control comprises two nested closed loops. The inner and faster loop corresponds to stator currents and the outer and slower one corresponds to torque, and thus to the interchanged power [21]. Feedforward current control can also be used provided a sufficiently accurate model is available, to avoid closed loop stability issues, as electrical machine dynamics are inherently stable [22]. The control commands the proper current references producing the required torque and leading to the maximum energy efficiency at steady state [20,22].

The electrical machine is usually controlled to vary the torque as needed in order to keep the DC-link voltage constant. This is achieved by ordering motor/brake torque to accelerate/decelerate flywheel when the DC-link voltage rises/falls. Hence, the constant voltage DC-link behaves as an ideal DC voltage source analogous to a conventional electrochemical battery.

In order to connect the FESS to an AC grid, another bidirectional power converter (DC/AC), usually referred as rectifier, is necessary. Most of the times another three-phase bridge of semiconductor switches [16,20] is used with a capacitor acting as DC-link [7], see Fig. 1. Higher switching frequency reduces the current ripple, easing the connection filter design, and increases the rectifier control bandwidth, but again at expense of increased switching losses. The rectifier allows supplying/retrieving active and reactive power to/from the AC grid with sinusoidal currents. The rectifier connected to the constant voltage DC-link establishes current references to produce/consume the required active and reactive power. The above-mentioned control, which will be used for the later simulation, contrasts with usual servo control for the electrical machine. For the servo case, the rectifier controls DC-link voltage to be constant and the inverter commands the torque references for speed control. This scheme has also been used for FESS considering the interchanged power equal to the torque reference times the mechanical speed by neglecting all the losses [23].

2.5. Bearings

Conventional mechanical bearings are a source of energy losses, need lubrication and require periodic maintenance due to wearing. In order to avoid these limitations FESSs make use, totally or partially, of magnetic bearings, where the shaft levitates due to repulsive magnetic forces. As there is no friction, there is no wearing either, resulting in almost no maintenance. Indeed, there is no need of lubrication, which results appropriate for absolute vacuum confinements. FESSs still need auxiliary mechanical bearings in case of the failure/overload in magnetic bearings [3].

Passive magnetic bearings consist of permanent magnets and must be combined with another type of bearings as they are inherently unstable. Active magnetic bearings consist of coils that vary the electromagnetic forces based on the shaft position attaining stability by using a feedback system. Finally, magnetic bearings based on superconductors take advantage of the diamagnetic behavior of superconductors when the superconduction temperature is reached by means of a criogenization system [24].

2.6. Enclosure

The aerodynamic friction torque is proportional to the spinning speed and to the density and pressure of the gas surrounding the flywheel. In order to reduce the aerodynamic losses, the flywheel is confined in a vessel with partial vacuum (reduced pressure) or with a gas less dense than the air, e.g. Helium [3]. In order to completely eliminate the aerodynamic losses, the flywheel is confined into a vessel with absolute vacuum, which makes difficult the electrical machine cooling and the mechanical bearings lubrication.

The enclosure must be capable of withstanding the impacts of the flywheel fragments in case of accidental destruction due to overspeed. Composite material fibers disintegrate progressively in numerous fragments, with mainly rotational movement, easy to be retained by the enclosure as their energy is dissipated by friction. Steel explodes violently in a few fragments, with mainly translational movement, difficult to be retained by the enclosure [8]. Therefore, high-speed FESSs require an enclosure weighing half the flywheel weight whereas low-speed FESSs two and half times for the very same stored energy amount [1].

2.7. FESS components research and development needs

High-speed FESSs still have high costs that limit widespread adoption. The main areas for advancement are those related to the flywheel material and the magnetic bearings [25]. The FESS energy density should be increased by using higher performance materials at lower cost [26]. Manufacturers need further research to identify the optimum conditions for the fabrication process of the carbon fiber-reinforced plastics determining the ideal temperatures of the resin and mandrel, winding speed of the fibers, and winding patterns [25]. In addition, accurate models of the composite flywheels should be developed to predict the long-term operation and assessing the system health. These models will have to consider creep, fatigue, and fracture tendencies of the material.

Improvements to the homogeneity of the magnetic field distribution in superconducting magnetic bearings will reduce the rotation loss by mitigating eddy currents that lead to inefficiency and material fatigue. Moreover, effectiveness in handling flux creep of the superconducting material should be developed to avoid the gradual fall from decreased levitation forces. Finally, active magnetic bearings need additional efforts to reduce their rotation losses and energy consumption [25,27].

3. FESS main applications

An FESS can be used as ESS for short-term since it allows continuous variations in the interchanged power with fast response and long lifespan. In [3,28,29] FESSs are compared with other short-term and long-term ESS. FESSs are typically employed in transportation and power quality applications as both require a large number of charge–discharge cycles [30]. Low-speed FESSs are only appropriate for stationary applications related to power quality where the specific energy is not important. FESSs are also used in the aerospace industry [3,31].

3.1. Applications related to power quality

Uninterruptible power system (UPS) is the most successful application for FESSs. This is because 97% of AC outages last less than 3 s [7] and they are more reliable than traditional sealed lead–acid batteries. In addition, the standby generators can reliably support the critical load in 10 s or less. FESS replaces electrochemical batteries in the UPS whatever its configuration is (on-line, off-line, etc.) [7]. It can be considered that FESS is a mature technology with many manufacturers in the market [2].

In electrical systems, the power supply and demand varies from second to second. In each instant if the produced power is higher/lower than the consumed load the system frequency rises/drops. This effect is increased by the growing presence of renewable power sources (wind and solar) with intermittent production [32]. Hence, the system operator needs controllable power sources, usually fossil fuel powered plants, for frequency regulation [33]. The use of ESSs allows increasing the renewable energy penetration and in [34] several energy storage technologies including FESS are reviewed for wind power applications. The reliability, long useful life and quick response of the FESS allows using it for frequency regulation without burning fossil fuel and therefore no produced emissions. In Stephentown, NY, a FESS-based plant storing 20 MW during 15 min is used for frequency regulation. The plant can consume/produce 20 MW according to the current needs with response time of less than 4 s. The plant comprises more than 200 flywheels and each flywheel weights 1150 kg and spins magnetically levitated at 16×10^3 rpm [35]. The direct competition for FESS-based plants for frequency regulations are those based on Li–ion batteries. These plants based Li–ion batteries are more inexpensive to install but the extremely fast cycling requirements might limit the depth of discharge and degrade the energy storage capability [36].

FESSs have also been used in isolated power systems. The island of Utsira–Norway [37] is supplied by a wind/hydrogen plant which includes an 100 kVA grid forming synchronous machine and a 200 kW output power low-speed FESS with an energy storage capacity of 5 kWh used as a short-term storage to compensate the seconds range wind energy fluctuations. The power system of the island of Flores–Azores [38] has a mix of diesel, wind and hydro generators and includes a 350 kW output power/5 kWh capacity FESS with the main function of improving system frequency stability. The wind diesel hybrid system (WDHS) of Coral Bay, Australia, combines seven diesel generators, each 320 kW, with three wind turbines, each 275 kW. The WDHS uses a FESS that produces/consumes 500 kW and stores 5 kWh to smooth the fluctuating the wind power [39].

3.2. Applications related to traction

In traction engines, there exist an average and fluctuating power consumption due to the accelerations and decelerations. The propulsion source is usually oversized to be capable of coping with the maximum power consumption during accelerations and the regenerative braking energy is usually dumped. More efficient

it is to size the main propulsion source for the average power consumption and allow ESS systems coping with the fluctuating power consumption. The ESS stores energy during braking periods, which will be supplied back during the accelerations [31]. In hybrid vehicles the main power source is a motor of internal combustion [3,6], and by means of the ESS, reductions in the fuel consumption, emissions and maintenance are achieved. Whereas most of the hybrid cars use electrochemical batteries as ESS (Ni–MH for middle range and Li–ion for high-end vehicles) [40] advanced sport cars are using FESS [41,42], again, due to the extreme cycling requirements. Analogous benefits are obtained when this procedure is applied to trains whose propulsion source is a gas turbine. When used in applications related to traction, flywheels act as gyroscopes offering resistance to change the rotation axis orientation. In order to remove this effect, flywheels must be mounted within a set of gimbals or controlled as pairs spinning synchronously in opposite directions [3].

Using FESS to improve the power quality in the catenaries of subway and electric trains is halfway between applications related to power quality and traction. FESS mitigates voltage oscillations in the catenaries and reduces the total electricity consumption by recovering the energy coming from regenerative braking otherwise dumped. In addition, substations for supplying stations of new construction can be sized only for the average power consumption with FESS coping with the fluctuating power in a manner analogous to the one previously explained [3].

3.3. Applications related to aerospace industry

Satellites use electrochemical batteries that are charged during the periods of light by means of solar panels and discharged during the periods of darkness. When replacing the electrochemical batteries by a FESS, mass and volume reductions are obtained along with increased reliability in the SOC monitoring and longer useful lifetime. Even more weight and volume reductions are possible if the FESS have a double function: energy storage and the satellite orientation control. The FESS also are used to provide the power pulse to the new electromagnetic systems for launching airships in aircraft carriers replacing heavier and less efficient steam storage-based catapults [31].

4. Application of a FESS to an isolated wind power system

In this section the isolated wind power system (IWPS) with a FESS shown in Fig. 3 is simulated. The IWPS of Fig. 3 can be considered a high penetration WDHS in wind only mode where the diesel generators are not running and only the WTGs supply active power to the system [43,44]. It comprises one WTG which supplies uncontrolled active power, a consumer load which consumes uncontrolled active power, a FESS which consumes/generates controlled active power and a synchronous machine (SM). The SM generates the voltage waveform and its voltage regulator controls that the voltage is within prescribed levels. For this reason the SM must be always running close to its rated speed. In the system to simulate only one WTG is considered so that the wind power fluctuation is maximum corresponding to the worst conditions for the FESS. In a system with N WTGs, the localized wind turbulence is smoothed by the spatial dispersion of WTGs and for well dispersed WTGs, the standard deviation of short-term wind power fluctuations can be reduced by a factor of up to \sqrt{N} [45].

The IWPS of Fig. 3 can only work if the average power coming from the WTG is greater than the power consumed by the load (plus a safety margin). The frequency is regulated by maintaining the instantaneous balance of the active power consumed and

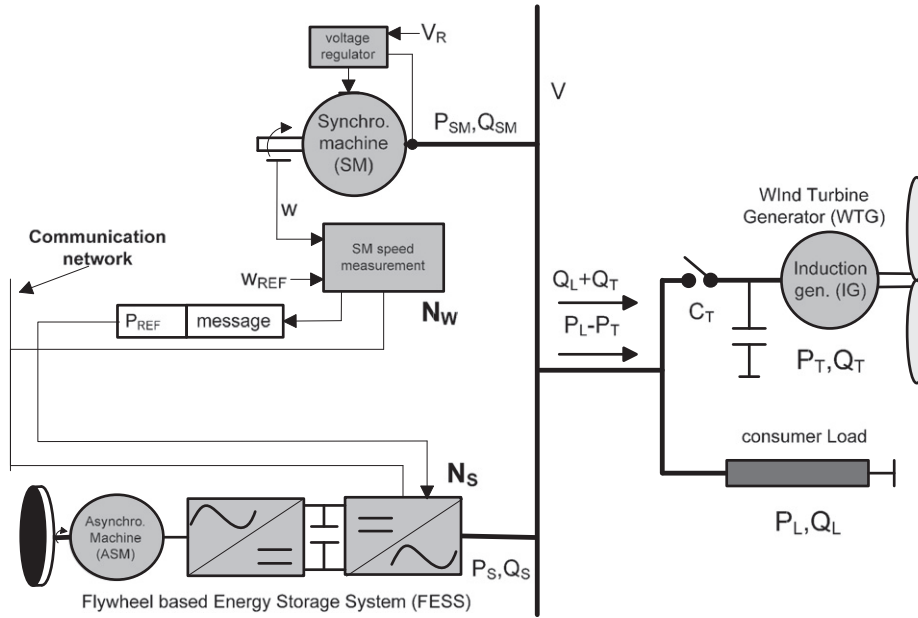


Fig. 3. IWPS with FESS and DCS considered in the paper.

produced. To accomplish this active power balance, the FESS can store ($P_S > 0$) the surplus active power from the WTG or retrieve power ($P_S < 0$) in the periods when the wind power is less than current load. If P_T ($P_T > 0$) and P_L ($P_L > 0$) are respectively the active power generated by the WTG and consumed by the load, J is the inertia of the SM, and ω is the SM shaft speed in rad/s (related to the frequency of the voltage waveform f by $\omega = 2\pi f/p$, with p the SM number of pole pairs), the power equation of the IWPS if no losses are taking into account is

$$P_T - P_L - P_S = J\omega \frac{d\omega}{dt} \quad (5)$$

$$\frac{d\omega}{dt} = 0 \Rightarrow P_T - P_L = P_S \quad (6)$$

Eq. (6) shows that to obtain constant synchronous shaft speed (system frequency) ($d\omega/dt=0$), the FESS must consume power when P_T exceeds P_L and the FESS must generate power when P_T is less than P_L .

Fig. 3 shows a distributed control system (DCS) consisting of two CPU-based electronic control units (also called nodes) physically distributed and linked by a communication network. This DCS is in charge of controlling the system frequency.

As it can be seen in Fig. 3, the two nodes are: the SM shaft speed measurement sensor node N_W and the actuator node N_S controlling the FESS. To control system frequency the node N_W calculates a PID frequency regulator whose input is the frequency error (difference between the current frequency and the power system nominal frequency 50/60 Hz) and whose output is the reference power P_{REF} needed to be absorbed/supplied ($P_{REF} > 0$ / $P_{REF} < 0$) by the FESS to balance the active power of the system. The power reference values P_{REF} are sent by means of the periodic message shown in Fig. 3.

5. IWSP with FESS simulation schematics

The Matlab-Simulink [46] model of the WDHS of Fig. 3 is shown in Fig. 4. Some of the components described next such as the WTG-induction generator (IG), the SM and its voltage regulator, the consumer load, the 3PB breaker, the FESS-ASM, the

elevating transformer, etc., are blocks which belong to the SimPowerSystems [47] library for Simulink.

The sixth-order model SM has a rated power (P_{SM-NOM}) of 300 kVA. Its mechanical input power is 0, so it runs freely behaving as a synchronous condenser and has an inertia constant of 1 s. An IEEE type 1 voltage regulator plus an exciter regulates the voltage in the SM terminals.

The constant speed stall controlled WTG [48] consists of a fourth-order model induction generator (IG) of 275 kW (WTG rated power $P_{T-NOM}=275$ kW) directly connected to the autonomous grid and the wind turbine (WT) block. The WTG has an inertia constant of 2 s. The WT block contains the wind turbine characteristic which defines the mechanical torque applied to the IG as a function of the wind speed and the IG shaft speed. The WT used has no pitch control, so there is no way to control the WTG active power. Since the WTG active power depends among other factors on the cube of the wind speed [49], all the wind speed variabilities are transmitted to the WTG active power, so the selected WTG results in the worst case of wind power variability to be balanced by the FESS. On the other hand, the used WTG has robust construction, low cost and simply maintenance and these are important factors in the remote locations of WDHS. The IG consumes reactive power so a capacitor bank has been added to compensate the power factor.

5.1. FESS description and sizing

The simulated FESS is a low-speed type consisting of a steel flywheel driven by an asynchronous machine (ASM) as a reduced weight is not important for stationary applications. Also as WDHSs are situated in remote locations, low cost and simple maintenance of the FESS are important factors, so the ASM is selected because of its robust construction, low cost, wide availability and high torque and the steel flywheel is selected because of its low cost and simple manufacture [50]. The 8 kHz switching frequency rectifier has a rated power of 150 kW and works with unity power factor to minimize its size, so the FESS behaves as a 150 kW controlled sink/source of active power. The FESS reference of active power P_{S-REF} can be established to operate in generating mode ($P_{S-REF} < 0$, the FESS decelerates the flywheel

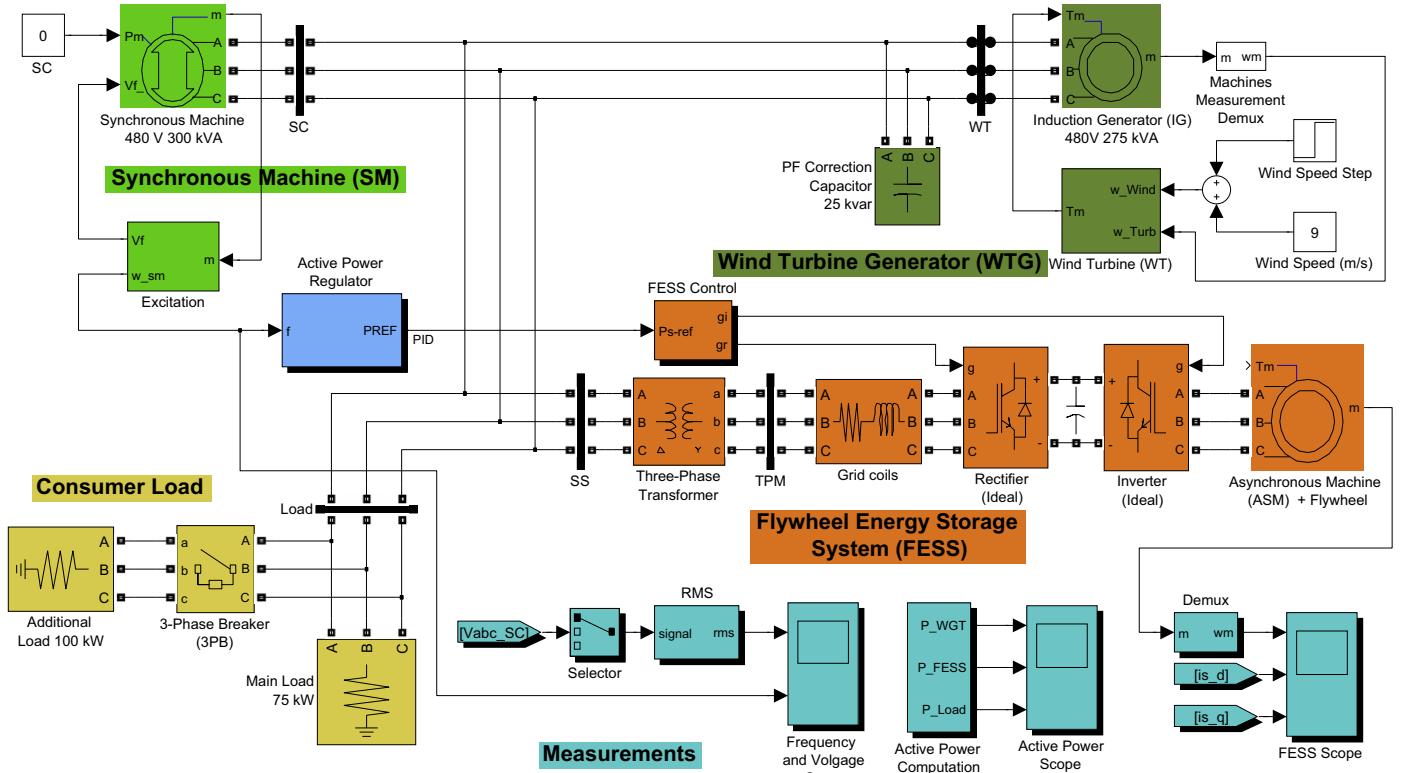


Fig. 4. MATLAB-Simulink schematic of the IWPS with FESS.

by supplying power to the isolated grid), or in motoring mode ($P_{S-REF} > 0$, the FESS accelerates the flywheel by absorbing power from the isolated grid). The transformer with ratio 1:1 isolates the FESS from the autonomous grid [47]. The DC-link voltage $V_{DC} = 800$ V and the 4.7 mF capacitance of the electrolytic capacitor bank for the DC-link allow the exchange of 150 kW with additional voltage margin to improve the current control dynamics.

The number of pole pairs in the asynchronous machine is only one so it is able to reach elevated speeds [5]. The maximum speed for the flywheel can be chosen near the rated speed ω_{mn} of the single pole pair ASM (3000/3600 rpm for 50/60 Hz rated grid frequency) in order to use conventional bearings. The minimum flywheel speed cannot be near zero because the FESS rated power must be exchanged independently of the speed and the needed torque for low speeds would result too high ($P = T\omega$). Therefore, as commented previously half the rated speed $\omega_{mn}/2$ is selected as minimum speed [51] for the flywheel in order not to oversize the electrical machine. For the rated speed $P_n = T_n\omega_{mn}$ where P_n and T_n are the rated power and the rated torque of the ASM. Hence, for the selected minimum speed $\omega_{mn}/2$ in order to exchange the rated power $150 \text{ kW} = T_n\omega_{mn}/2 = P_n/2$, and so the required ASM rated power is 300 kW. An example of ASM that meets these requirements can be found in [52].

In a WDHS the start-stop cycling frequency of the diesel generators due to the intermittent nature of the wind decreases from the very first minute of the average load storage in the ESS [53]. If the 150 kW FESS rated power is considered the average load of the IWPS, the necessary storage energy in the FESS by selecting 2 min of average load corresponds to $150 \text{ kW} \times 120 \text{ s} = 18,000 \text{ kJ}$. The energy available in the FESS with speed ranging from ω_{mn} to $\omega_{mn}/2$ is

$$E_c = \frac{1}{2} I \left[\omega_{mn}^2 - \left(\frac{\omega_{mn}}{2} \right)^2 \right] = \frac{3}{4} \left(\frac{1}{2} I \omega_{mn}^2 \right) \quad (7)$$

Therefore, the moment of inertia for a flywheel with speed range spanning from 3600 rpm to 1800 rpm so that the stored energy is 18,000 kJ corresponds to $I = 338 \text{ kg m}^2$ according to (7). This calculated inertia is entered as the inertia parameter of the FESS-ASM of Fig. 4, so that the ASM simulates also the flywheel. In a flywheel made of steel ($\rho = 7800 \text{ kg/m}^3$ [10]) and disk-shaped ($r_i = 0$), the required radius to obtain $I = 338 \text{ kg m}^2$ corresponds to $r_o = 0.620 \text{ m}$. These calculations have been done for a proportion between disk thickness and radius of 0.3 so that the planar stress condition is maintained [10]. The resulting weight of the flywheel is 1.76 Tm. The maximum hoop stress occurs in the center of the disk and is equal to 352 MPa and 176 MPa for the disc with hole (infinitesimal radius) and without hole, respectively, which corresponds to 2.3 and 4.5 times lower than the ultimate stress for steel $\sigma_u = 800 \text{ MPa}$ [10], so that for safety reasons the no hole solid disc of Fig. 2 must be used. For other characteristic shapes of the metallic flywheels, the results are very similar. There are readily available commercial flywheels with similar characteristics to these described in here [50].

Field oriented control (FOC) is used to obtain high performance in the dynamic control of the ASM. The FOC allows decoupled control of flux and torque of the ASM in a manner analogous to that of the DC machine [54]. The rotor flux $\Psi_r = L_m i_{mr}$ (L_m and i_{mr} are the magnetizing inductance and current, respectively) is produced by the stator direct current i_{sd} and its dynamics is limited by the presence of the elevated rotor time constant $T_r = L_r/R_r$ (L_r and R_r are the rotor inductance and resistance, respectively). The electromagnetic torque is the product of the rotor flux and the stator quadrature current i_{sq} . The FOC keeps a constant rotor flux (slow dynamics) at its optimal value and quickly varies the torque (fast dynamics) by means of the quadrature current i_{sq} . Finally, the rotor flux should be reduced in order to achieve high speeds once the inverter voltage ceiling is reached. The structure for FOC in the ASM

consists of cascaded or nested controls [55]. This control structure allows protecting the converter and machine as the current references can be limited [55].

6. IWPS with FESS simulation results

In the graphs presented below the system frequency and the rms voltage are plotted in pu value in Figs. 5 and 6 respectively. The active powers (kW) for the WTG, consumer load and FESS are plotted in Fig. 7 and they are considered positive/negative when they are produced/consumed. Fig. 8 shows the variables for the FESS: ASM speed, direct current and quadrature current. At the starting point in $t=0$ s, the active powers consumed by the load and FESS are 75 and 68 kW, respectively. The wind speed is 9 m/s and the active power produced by the WTG is 143 kW, being the system in steady state.

6.1. Load step

Starting at the described initial state, a positive step of 100 kW in the consumer load is applied at $t=0.2$ s. by closing the three phase breaker 3PB shown in Fig. 4, so that the total load (175 kW) is greater than the WTG produced power. Fig. 7 shows the load step, how the FESS active power changes from -68 kW (consuming) to 32 kW (supplying) and a transient in the WTG active power with minimum and maximum during oscillations of 130 and 232 kW respectively. During the transient due to the load step the minimum frequency pu is 0.9985 (Fig. 5) and the minimum and maximum RMS voltage pu are 0.9892 and 1.0028 respectively (Fig. 6). In the steady state reached at $t=1.721$ s, the WTG produced active power stays at the same initial value (143 kW) as the wind speed has not changed and the FESS supplies the active power deficit to the consumer load.

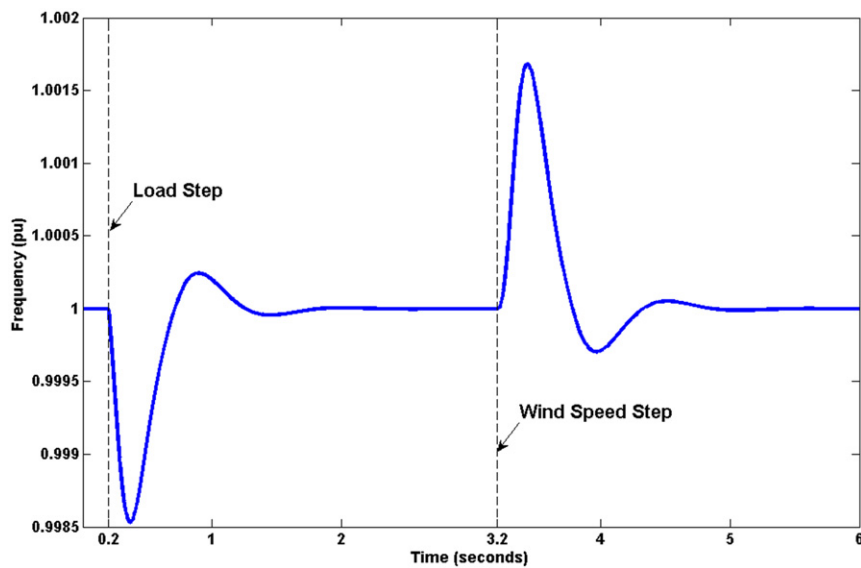


Fig. 5. System frequency per unit.

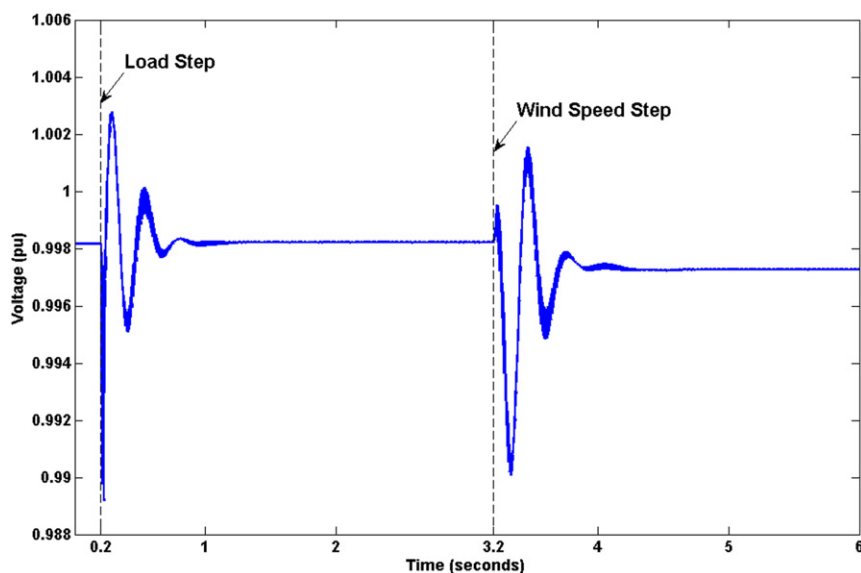


Fig. 6. System voltage per unit.

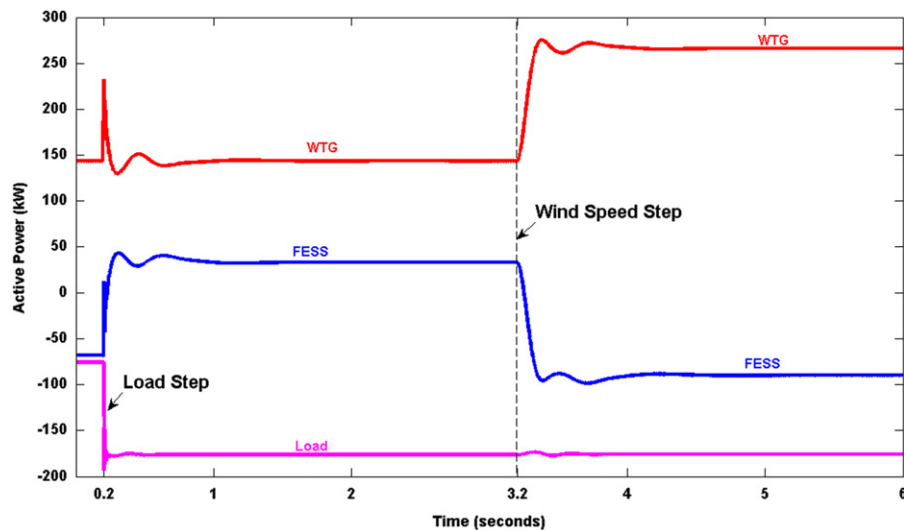


Fig. 7. WTG, FESS and load active power (positive when produced).

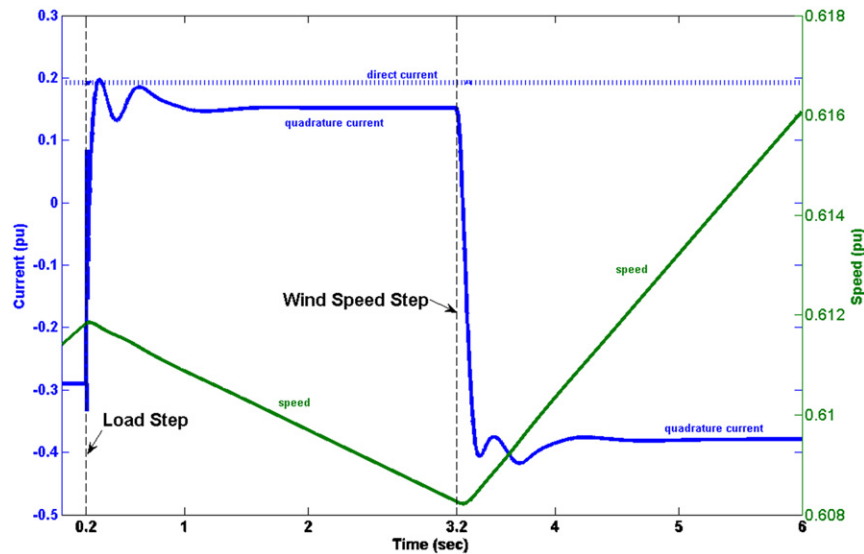


Fig. 8. Normalized ASM speed and direct and quadrature currents.

6.2. Wind step

In $t = 3.2$ s, the wind speed changes from 9 to 11 m/s. The power produced by the WTG increases and reaches 266 kW in steady state (a 99% increase in wind power in relation to its initial value at $t=0$). During the transient due to the wind step change, the f_{pu} minimum/maximum are 0.9997/1.0017 pu, see Fig. 5 and the voltage pu minimum/maximum are 0.9901/1.0015 pu, see Fig. 6. In $t = 4.805$ s, the transient finishes with the FESS consuming the wind power excess 91 kW.

The ASM direct and quadrature stator currents and the flywheel shaft speed are shown in pu values in Fig. 8 (base current value is 709.46 A and base speed is 3600 rpm). The direct current, which controls the magnetic flux, has always a positive sign. The quadrature current, which controls the electromagnetic torque, has a positive (negative) sign for brake (motor) torque, decreasing (increasing) the flywheel speed, and with the FESS supplying (consuming) power to the isolated grid. This

quadrature current sign criterion is the opposite of the usually employed with servos. In Fig. 8 the magnetizing current and therefore the direct current keeps constant in 0.19 pu, optimum value with maximum power factor at rated power. This is because the flux weakening mechanism does not act as the DC link provides enough voltage ceiling [55]. Thus, the electromagnetic torque varies only due to the ASM quadrature current. Neglecting all the losses, the FESS active power can be approximated to the ASM electromagnetic torque times the flywheel speed. The flywheel speed barely varies because of the relatively high inertia and the reduced simulation time. Therefore, FESS active power is directly proportional to the ASM quadrature current. This explains that the ASM quadrature current in Fig. 8 resembles a scaled version of the FESS active power in Fig. 7. In Fig. 8 the quadrature current is initially -0.29 pu with the FESS absorbing power from the isolated grid. After the load step, the quadrature current increases to 0.15 pu so the FESS provides the necessary power to the isolated grid for satisfying the increased demand.

After the positive step change in the wind speed, the quadrature current turns negative again -0.38 pu and the FESS absorbs the wind power excess.

The flywheel speed is initially increasing, as the FESS is absorbing power. At $t=0.2$ s. the flywheel speed is 0.6118 pu and, after the load step, starts to reduce as the FESS supplies power to the isolated grid at the expense of its stored mechanical energy. This reduction is approximately linear as the supplied power, and so the brake torque, is approximately constant. Finally, after the wind speed step at $t=3.2$ s, the flywheel speed, at that point 0.6083 pu, increases linearly as now the FESS absorbs the wind power excess. At the end of the simulation at $t=6$ s the flywheel speed is 0.6161 pu.

7. Conclusions

The components that form an FESS: bidirectional converter, electrical machine, flywheel, bearings and enclosure have been reviewed. Also the main applications of FESS: power quality, traction and aerospace are presented. FESSs are suitable for interchanging medium to high powers (kW–MW) during short periods (seconds–minutes) so that they can be used as a short-term ESS in power systems. The allowable number of charge and discharge cycles is very elevated (hundreds of thousands) and it is independent of the temperature and the SOC. These characteristics made the FESSs adequate to be used in isolated power systems, such as the presented IWPS in sections 4–6, for smothering the power oscillations. Indeed, the remote locations of the isolated power systems call for a low-speed FESS with low cost steel flywheel, robust asynchronous machine and mechanical bearings. Low-speed FESSs are 3–5 more inexpensive than high-speed FESSs [7] and Ref. [56] estimates that the purchase cost of a low-speed FESS is about \$100/kW and that for high-speed FESS is about \$300/kW.

Supported by all the material shown in Section 2, in Section 5 it is presented the sizing of a FESS with low-speed range (1800–3600 rpm) and able to supply 150 kW during 2 min consisting of a 300 kW ASM and a 1.76 Tm steel flywheel. Simulations show that the sized FESS properly smoothes the IWPS power variations. The response to the $+100$ kW load step shows a frequency falling of -0.15% , a 1.36% voltage variation, the FESS changing from loading to generating power and a settling time of 1.521 s. During the $+2$ m/s wind speed step, the frequency rises up to 0.17% , the voltage variation is 1.14% , the FESS returns to consume the wind power excess and the settling time is 1.605 s. The simulations have also the aim of supporting explained concepts of Sections 2 and 5 by presenting the variables of the FESS: ASM direct current which controls the magnetic flux and is kept constant, ASM quadrature current, which controls the electromagnetic torque and resembles a scaled version of FESS active power and the flywheel speed which indicates the FESS stored energy and increases/decreases almost linearly as the accelerating/braking torque during simulations can be considered nearly constant.

References

- [1] Holm SR. Modelling and optimization of a permanent magnet machine in a flywheel. PhD thesis. Delf University of Technology, Netherlands; 2003.
- [2] Ruddell A. Investigation on storage technologies for intermittent renewable energies: evaluation and recommended R&D strategy. Investire-network storage technology report ST6: flywheel. Contract no. ENK5-CT-2000-20336; 17 June 2003 <http://www.itpower.co.uk/investire/pdfs/flywheel_rep.pdf>.
- [3] Hebner R, Beno J, Walls A. Flywheel batteries come around again. IEEE Spectrum 2002;39(4):46–51.
- [4] Plater B, Andrews JA. Advances in flywheel energy-storage systems. Power-Pulse.net by Darnell.Com Inc 2001.
- [5] Bolund B, Bernhoff H, Leijon M. Flywheel energy and power storage systems. Renewable and Sustainable Energy Reviews 2007;11(2):235–58, <http://dx.doi.org/10.1016/j.rser.2005.01.004>.
- [6] Hayes RJ, Kajs JP, Thompson RC, Beno JH. Design and testing of a flywheel battery for a transit bus. In: 1999 SAE international congress and exposition, Detroit, MI; 1–4 March 1999.
- [7] Emadi A, Nasiri A, Bekiarov SB. Uninterruptible power supplies and active filters. first ed. CRC Press; 28 October 2004.
- [8] Sapowith AD, Handy WE. A composite flywheel burst containment study. Technical report AVSD-0350-81-RR. Lawrence Livermore National Lab; 8 April 1982.
- [9] Genta G. Kinetic energy storage: theory and practice of advanced flywheel systems. Butterworth-Heinemann Ltd.; February 1985.
- [10] Wagner HD. Design example#2: advanced composite flywheel. In: Lectures on composite materials. Weizmann Institute of Science, Israel; 2009.
- [11] Thoolen FJM. Development of an advanced high speed flywheel energy storage system. PhD thesis. Eindhoven University of Technology, Eindhoven, The Netherlands, DecFBESer; 1993.
- [12] Jiancheng Zhang, Zhiye Chen, Lijun Cai, Yuhua Zhao. Flywheel energy storage system design for distribution network. In: Power engineering society winter meeting, vol. 4. IEEE 2000. p. 2619–23.
- [13] Yoon-Ho Kim, Kyoung-Hun Lee, Young-Hyun Cho, Young-Keun Hong. Comparison of harmonic compensation based on wound/squirrel-cage rotor type induction motors with flywheel. In: Power electronics and motion control conference. Proceedings of the PIEMC 2000, vol. 2. The Third International Published; 2000. p. 531–36.
- [14] Akagi H, Sato H. Control and performance of a doubly-fed induction machine intended for a flywheel energy storage system. IEEE Transactions on Power Electronics 2002;17(1):109–16.
- [15] Seok-Myeong Jang, Sang-Sub Jeong, Dong-Wan Ryu, Sang-Kyu Choi. Comparison of three types of PM brushless machines for an electro-mechanical battery. IEEE Transactions on Magnetics 2000;36(5):3540–3.
- [16] Iglesias LJ, Garcia-Tabares L, Agudo A, Cruz I, Arribas L. Design and simulation of a stand-alone wind-diesel generator with a flywheel energy storage system to supply the required active and reactive power. In: Power electronics specialists conference, 2000 PESC 00, vol. 3. 2000 IEEE 31st Annual Published; 2000. p. 1381–86.
- [17] Hofmann H, Sanders SR. Optimal efficiency controller for synchronous reluctance flywheel drive. In: Telecommunications energy conference, 1998. INTELEC. Twentieth International 1999. p. 724–31.
- [18] Liuchen Chang. Comparison of AC drives for electric vehicles—a report on experts' opinion survey. IEEE Aerospace and Electronic Systems Magazine 1994;9(8): 7–11.
- [19] Ehsani M, Yimin Gao, Gay S. Characterization of electric motor drives for traction applications. In: Industrial Electronics Society, 2003. IECON '03. The 29th annual conference of the IEEE, vol. 1; 2–6 November 2003. p. 891–96.
- [20] Hofmann H, Sanders SR. Synchronous reluctance motor/alternator for flywheel energy storage systems. IEEE Power Electronics in Transportation 1996;199–206(March):24–5.
- [21] Santiago W. Inverter output filter effect on PWM motor drives of a flywheel energy storage system. In: Second international energy conversion engineering conference sponsored by the American Institute of Aeronautics and Astronautics, Providence, RI; 16–19 August 2004.
- [22] Park JD, Khalizadeh C, Hofmann H. Design and control of high-speed solid-rotor synchronous reluctance drive with three-phase LC filter. In: Industry applications conference, 2005. Fortieth IAS annual meeting conference record of the 2005, vol. 1; 2–6 October 2005. p. 715–22.
- [23] Hardan F, Bleijs JAM, Jones R, Bromley P. Bi-directional power control for flywheel energy storage system with vector-controlled induction machine drive. In: Power electronics and variable speed drives, 1998. Seventh international conference on (conf. publ. no. 456); 21–23 September 1998. p. 477–82.
- [24] Siebert M, Ebihara B, Jansen R, Fusaro RL, Morales W, Kascak A, et al. A passive magnetic bearing flywheel. In: Glenn technical report NASA/TM-2002-211159; February 2002.
- [25] Elkin E, et al. Final project report: 2020 strategic analysis of energy storage technologies; August 2011. University of California, Berkeley School of Law; University of California, Los Angeles; University of California, San Diego; Prepared for: CIEE.
- [26] Shaobo Wen, Shuyun Jiang. Optimum design of hybrid composite multi-ring flywheel rotor based on displacement method. Composites Science and Technology 2012;72(9):982–8, <http://dx.doi.org/10.1016/j.compscitech.2012.03.007>.
- [27] Ji-Yi Shen, Brian C. Fabien. Optimal control of a flywheel energy storage system with a radial flux hybrid magnetic bearing. Journal of the Franklin Institute 2002;339(2):189–210, [http://dx.doi.org/10.1016/S0016-0032\(02\)00021-2](http://dx.doi.org/10.1016/S0016-0032(02)00021-2).
- [28] Kondoh J, Ishii I, Yamaguchi H, Murata A, Otani K, Sakuta K, et al. Electrical energy storage systems for energy networks. Elsevier Energy Conversion & Management 2000;41(17):1863–74.
- [29] Ioannis Hadjipaschalis, Andreas Poullikkas, Venizelos Efthimiou. Overview of current and future energy storage technologies for electric power applications. Renewable and Sustainable Energy Reviews 2009;13(6–7):1513–22, <http://dx.doi.org/10.1016/j.rser.2008.09.028>.
- [30] Vazquez S, Lukic SM, Galvan E, Franquelo LG, Carrasco JM. Energy storage systems for transport and grid applications. IEEE Transactions on Industrial

- Electronics 2010;57(December (12)):3881–3895. <http://dx.doi.org/10.1109/TIE.2010.2076414>.
- [31] Haichang Liu, Jihai Jiang. Flywheel energy storage—an upswing technology for energy sustainability. *Energy and Buildings* 0378-7788 2007;39(5):599–604, <http://dx.doi.org/10.1016/j.enbuild.2006.10.001>.
- [32] Daim Tugrul U, Li Xin, Kim Jisun, Simms Scott. Evaluation of energy storage technologies for integration with renewable electricity: quantifying expert opinions. *Environmental Innovation and Societal Transitions* 2210-4224 2012;3:29–49, <http://dx.doi.org/10.1016/j.eist.2012.04.003>.
- [33] Rounds Robert, Peek Georgianne Huff. Design & development for a 20-MW flywheel-based frequency regulation power plant: a study for the DOE energy storage systems program. A study for the DOE energy storage systems. Technical report. Sandia National Laboratories; 2010.
- [34] Francisco Díaz-González, Andreas Sumper, Oriol Gomis-Bellmunt, Roberto Villafañila-Robles. A review of energy storage technologies for wind power applications. *Renewable and Sustainable Energy Reviews* 2012;(May (4)). p. 2154–71. ISSN 1364-0321, <http://dx.doi.org/10.1016/j.rser.2012.01.029>.
- [35] Smart energy matrix. 20 MW frequency regulation plant. Beacon Power <http://www.beaconpower.com/files/SEM_20MW_2010.pdf>.
- [36] Fairley P. Flywheels keep the grid in tune. *IEEE Spectrum* 2011;48(7):16–8.
- [37] Torgeir Nakken, Erik Frantzen, Elisabet F Hagen, Hilde Strøm. Utsira—demonstrating the renewable hydrogen society. *WHEC* 16/13–16 June 2006. Lyon France 1/10.
- [38] Hamsic N, Schmelter A, Mohd A, Ortjohann E, Schultze E, Tuckey A, et al. Increasing renewable energy penetration in isolated grids using a flywheel energy storage system. In: International conference on power engineering, energy and electrical drives. *POWERENG* 2007; 12–14 April 2007. p. 195–200.
- [39] Verve Energy. Coral bay wind diesel system—information sheet, Perth, Western Australia; February 2008.
- [40] Pistoia G. Electric and hybrid vehicles, power sources, models, sustainability, infrastructure and the market. first ed. Elsevier; 9780444535658.
- [41] Abuelsamid S. How it works: Porsche 911's GT3R hybrid flywheel. *Popular Mechanics* 2010.
- [42] Millikin M. Audi R18 e-tron quattro: diesel hybrid Le Mans racer with electric flywheel energy storage. In: Green car congress; 2012.
- [43] Sebastián R, Peña-Alzola R. Effective active power control of a high penetration wind diesel system with a Ni–Cd battery energy storage. *Renewable Energy* 2010;35(5):952–65, <http://dx.doi.org/10.1016/j.renene.2009.11.029>.
- [44] Sebastian R. Reverse power management in a wind diesel system with a battery energy storage. *International Journal of Electrical Power and Energy Systems* 2013;44(1):160–7, <http://dx.doi.org/10.1016/j.ijepes.2012.07.029>.
- [45] Welfonder E, Neifer R, Spanner M. Development and experimental identification of dynamic models for wind turbines. *Control Engineering Practice* 0967-0661 1997;5:63–73, [http://dx.doi.org/10.1016/S0967-0661\(96\)00208-0](http://dx.doi.org/10.1016/S0967-0661(96)00208-0).
- [46] The MathWorks, Inc.: Simulink (built upon Matlab). Online documentation <<http://www.mathworks.com/access/helpdesk/help/toolbox/simulink/>>.
- [47] The MathWorks, Inc.: SimPowerSystems. Simulink (built upon Matlab) block library online documentation <<http://www.mathworks.com/access/helpdesk/help/toolbox/phymod/powersys/>>.
- [48] Gagnon R, Saulnier B, Sybille G, Giroux P. Modelling of a generic high-penetration no-storage wind-diesel system using matlab/power system blockset. In: 2002 global windpower conference, Paris, France; April 2002.
- [49] Sebastián R, Peña Alzola R. Simulation of an isolated wind diesel system with battery energy storage. *Electric Power Systems Research* 2011;81(2):677–86, <http://dx.doi.org/10.1016/j.epsr.2010.10.033>.
- [50] Hamsic N, Schmelter A, Mohd A, Ortjohann E, Schultze E, Tuckey A, et al. Stabilising the grid voltage and frequency in isolated power systems using a flywheel energy storage system. In: The Great Wall World Renewable Energy Forum (GWREF), Beijing, China; October 2006.
- [51] Bernard N, Benahmed H, Multon B, Kerzreho C, Delamare J, Faure F. Flywheel energy storage systems in hybrid and distributed electricity generation. In: Conference and exhibition. *PCIM'03*, Nürnberg; May 2003.
- [52] ABB Ltd. Low voltage process performance NEMA frame motors. ABB/Cat. BU/ NEMA EN 04-2006 <[http://www05.abb.com/global/scot/scot234.nsf/veritydisplay/9b930a1e90aaea1ac125784f0037fb69/\\$file/lv%20nemamotor_s_en_04_2006.pdf](http://www05.abb.com/global/scot/scot234.nsf/veritydisplay/9b930a1e90aaea1ac125784f0037fb69/$file/lv%20nemamotor_s_en_04_2006.pdf)>.
- [53] Beyer HG, Degner T, Gabler H. Operational behaviour of wind diesel systems incorporating short-term storage: an analysis via simulation calculations. *Solar Energy* 1995;54(6):429–39.
- [54] Boldea I, Nasar SA. Vector control of AC drives. Ed. CRC; 26 August 1992.
- [55] Leonhard W. Control of electrical drives. second ed. Springer; 1996.
- [56] US Department of Energy. Flywheel energy storage: an alternative to batteries for uninterruptible power supply systems. Federal Technology Alert. DOE/EE-0286.